Journal of Engineering Technology and Applied Physics

The Integrated Simulation and Processing Tool for Ground Based Synthetic Aperture Radar (GBSAR)

Chee Siong Lim*, Voon Chet Koo and Yee Kit Chan
Faculty of Engineering and Technology, Multimedia University, Jalan Ayer Keroh Lama, 75450, Melaka, Malaysia
*cslim@mmu.edu.my
https://doi.org/10.33093/jetap.2019.1.2.5

Abstract - Ground-based Synthetic Aperture Radar (GBSAR) is a tremendous example of the extended applications of Synthetic Aperture Radar (SAR). GBSAR is extremely useful in human-made structure observations, terrain mapping, landslide monitoring and many more. However, the process of designing and developing the GBSAR system is rather costly and time-consuming. It would be of a great advantage for system designers to have a realistic simulation and designing tool to anticipate the results before the implementation of the final design. In this paper, we are going to present the integrated simulation and designing tool that we have developed for a generic GBSAR system. We named it iSIM v2.0.

Keywords—GBSAR, INSAR, SAR, simulation, processing

I. Introduction

Ground-based Synthetic Aperture Radar (GBSAR) is a tremendous extended application of Synthetic Aperture Radar (SAR) technique. GBSAR inherits the advantage of SAR in which it can work even without the presence of the sun since it can provide its illumination onto the area of interest. GBSAR typically moves along a finite length linear guide rail. The system transmits an electromagnetic wave, and the backscattering echo is collected as it progresses. The collected raw data can be processed to generate a SAR image with significantly improved resolution in the azimuth direction. The improvement due to the SAR technique is analogous to the effect of using a much longer antenna after taking advantage of the forward motion by the sensor. Similar to SAR, GBSAR is also a coherent imaging radar system. Exploiting the SAR images will extract various useful information of the targeted area. The cost of developing a GBSAR system relatively lower than that of airborne or space-borne SAR system, this has led to an increase in interest from various agencies to implement GBSAR technique in numerous applications such as human-made structure (bridge [1], dam [2], building [3], etc.) observation, terrain mapping [4], landslide monitoring [5] system and many more.

Design and development of a GBSAR system are time-consuming. The design and redesign loops could lead to unnecessary added costs to the project. A detailed and thorough system design and simulator tool will help in saving the time and cost in the system design stage. This paper presents the system design and simulator tool we have developed before kicking off with the actual system development.

II. Key Parameters of GBSAR

GBSAR system travels on a fixed-length linear guide rail shown in Fig. 1. The azimuth resolution of the output SAR images is directly proportional to the length of the linear guide rail. Increasing the length of the track will result in higher resolution SAR images in the azimuth direction. The bandwidth of the transmitted radio frequency, on the other hand, determines the fineness of the output SAR images in the range direction.
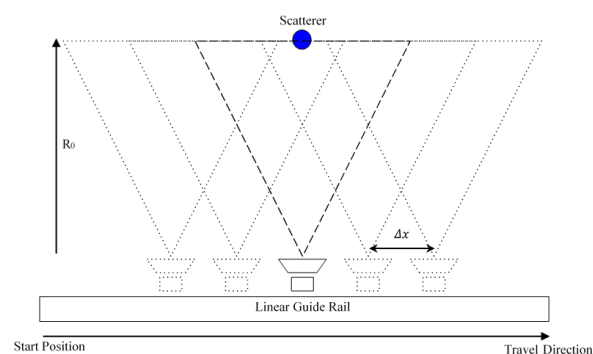
Fig. 1. Illustration of a GBSAR system.

The following Eqs. (1) – (3) show the maximum achievable resolution in both slant range δr and azimuth $\delta \theta_{az}$. The azimuth resolution is expressed in the term of radians and can be translated into the unit of meter δx by multiplying it with the distance to beam center R_0.

$$\delta r = \frac{c}{2B} \tag{1}$$

$$\theta_{az} = \frac{\lambda}{2L_s} \tag{2}$$

$$\delta x = \frac{\lambda R_0}{2L_s} \tag{3}$$

c is the speed of light approximated at 3×10^8 m/s. B is the transmitted signal bandwidth, λ is the signal wavelength, R_0 is the distance to beam center, and L_s is the synthetic aperture length.

These essential specifications need thorough consideration when designing a GBSAR system as they will determine the data volume, maximum reachable range, Eq. (4) and resolution of the output SAR image.

$$R_{max} = \frac{cN_y}{2B} \tag{4}$$

The balance between SAR image quality and the data processing load require trade-off decision making through some in-depth analysis. Therefore, a system design and simulator tool will come in handy for the system designer to save time and cost.

III. THE ISIM V2.0 DEVELOPMENT TOOL

iSIM v2.0 is developed in MATLAB. The program aims to simplify the process from system designing, signal simulation, signal processing, output analysis and system validation. The program has embedded various tools to assist the system designer at different stages in GBSAR design and development. Fig. 2 shows the overall flow chart of the program.
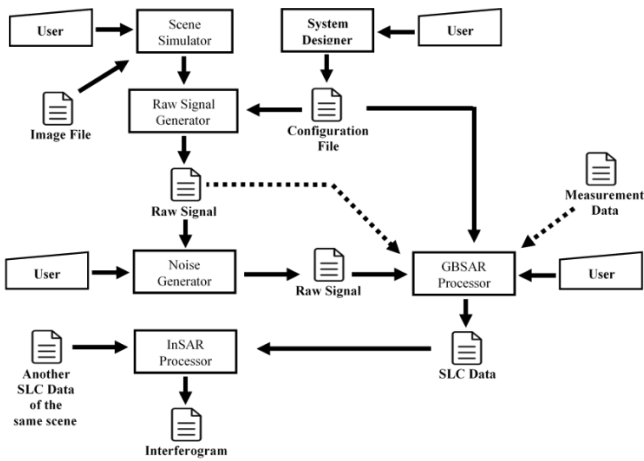
Fig. 2. Illustration of a GBSAR system.

A. System Designer

The first tool of the iSIM v2.0 is the system specification designer (Fig. 3). It allows the user to draft the desired specifications. User can input the parameters such as start frequency f_1, stop frequency f_2, frequency step count N_r, azimuth linear step count N_x, linear guide azimuth step size Δx, and the antenna length L_a. Based on these settings, the system designer module will calculate the wavelength λ,

slant range resolution δr, azimuth resolution δx, maximum reachable range R_{max}, antenna beam width θ_x, and the maximum azimuth coverage. The program will save these system parameters in the system configuration file for future use in the subsequent stages.
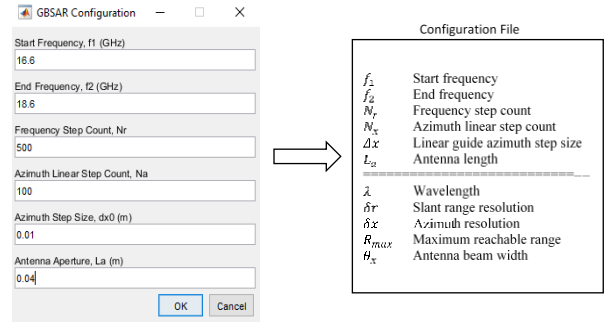
Fig. 3. iSIM v2.0 system designer GUI.

B. Raw Signal Generator

Another tool included in the program is the scene designer and raw signal generator. User can create a customised virtual scene terrain with the scene designer such as one shown in Fig. 4a. Besides, the user has the option to add point reflectors on top of the terrain surface. Apart from keying in the coordinates of the reflector targets manually, the sub-module also allows the user to import the image file (Fig. 4b) and translate it to the point targets (Fig. 4c). The emulated virtual scene with known targets is then generated, as shown in Fig. 4d (top view of the virtual scene) and Fig. 4e (3D view of the virtual scene).
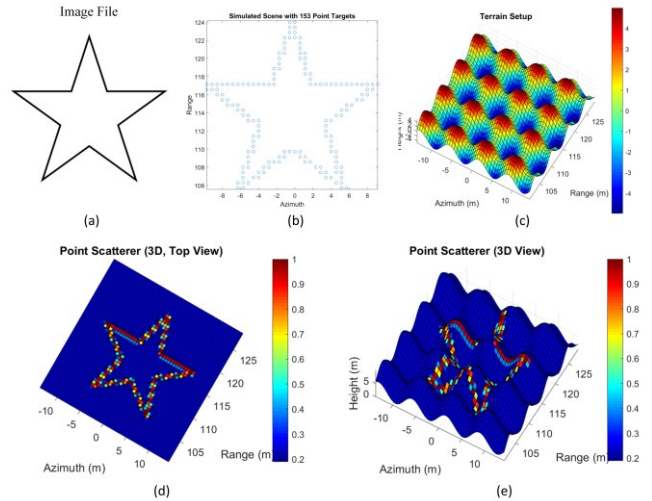
Fig. 4. Virtual scene simulation.

The return signal from N number of scatterers at coordinate (x_i, y_i, z_i) can be expressed in the form of Range frequency domain (range profile) as shown in Eq. (5).

$$S(x_n, w(t))$$

$$= \sum_{i=1}^{N} a_i e^{-j2w(t)\sqrt{(x_n - x_i)^2 + (y_a - y_i)^2 + (z_a - z_i)^2}} \tag{5}$$

a_i is the radar cross section (RCS) of the scatterer. $w(t)$ is the instantaneous radial frequency of the received signal. The antenna's coordinate is given as (x_n, y_a, z_a), where x_n is the nth azimuth position of the antenna on the linear guide rail. The variables y_a and z_a are the fixed position of the antenna in range and height direction, respectively. Fig. 5a illustrates part of the ten instantaneous simulated return signals from $x_n = -0.04m$ to $x_n = 0.05m$, with the distance of $1cm$ apart. Plotting the entire matrix of the simulated return signal of $S(x_n, w(t))$ will produce a raw image (unfocused) like one in Fig. 5b.
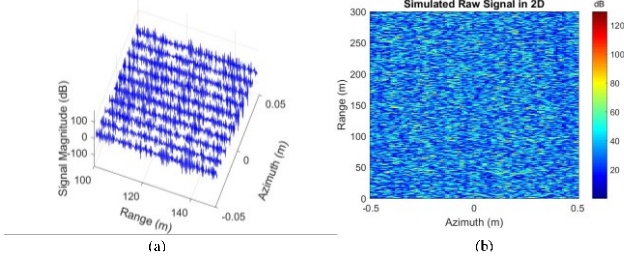
Fig. 5. GBSAR raw signal simulation.

The simulated signal in the GBSAR raw signal generator module is rather too ideal. It is almost impossible to achieve in real life as radio-frequency (RF) components are prone to noise in nature. Therefore, it is crucial to investigate the level of noise immunity of the system. White Gaussian noise can be added into the simulated raw signal. User can test and analyses the output image quality of the system with the different power level of the white Gaussian noise. Fig. 6 compares the original simulated return signal against the White Gaussian noise with SNR of 12.97dB and 7.97dB.
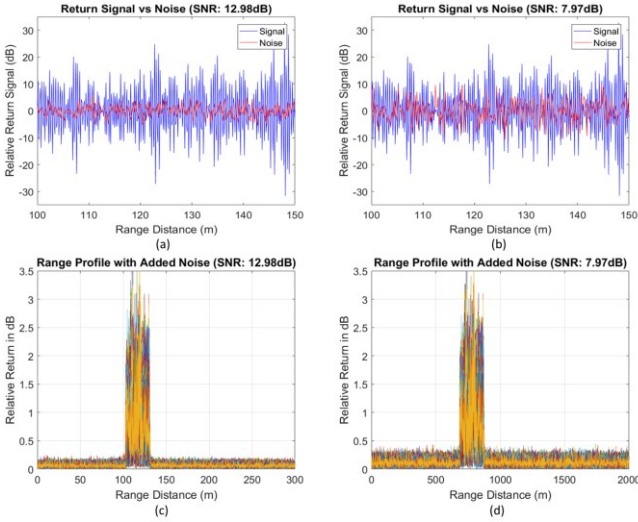
Fig. 6. Noise signal generation.

The process of simulating the raw signal could be time-consuming depending on the size of the virtual scene and the number of the simulated point targets. Therefore, The White Gaussian noise is added to the raw signal after the simulation process instead of adding it during the simulation process itself. The noise-added raw signal is saved in a separate file from the original (theoretical) return signal file. A new noise-added raw signal with different noise power level can be re-generated without having to repeat the entire simulation process.

C. Signal Processing Tool

iSIM v2.0 also comes with the GBSAR signal processing tool. It processes the raw signal to generate a single look complex (SLC) file. The GBSAR datasets are typically large in volume and usually requires very high computing power to process the entire dataset. Trimming the dataset can significantly reduce the processing load. This tool does support data trimming. Upon importing the raw signal, the program will display the range profile generated from the raw signal. The range profile provides valuable insight into deciding the distance range of interest to proceed with the GBSAR processing. From the range profile in Fig. 6c and 6d, there is some strong return appear between the range 100m and 135m, which is precisely the distance from the sensor to the simulated targets. Therefore, processing time can be reduced by cropping the data from the range 100m to 135m.
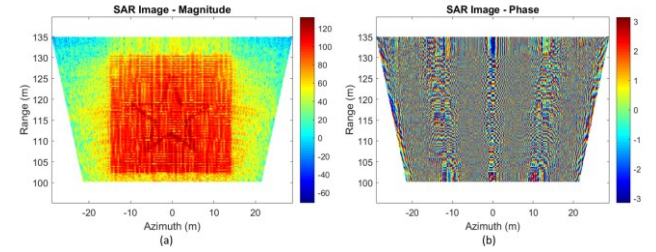
Fig. 7. SAR signal processing.

The technique adopted in this GBSAR signal processing tool is the Range Migration Algorithm (RMA) [6]. Fig. 8 shows the process flow of the RMA. Firstly, the raw data is Fourier transformed in the azimuth direction into (k_x, k_r) domain. The matched filter $S_{mf}(k_x, k_r)$ is then applied to the data. Before transforming the data back into the time domain, it is very crucial to correct the range curvature of the data matrix through Stolt interpolation. At this stage, the data will be interpolated in the k_r axis. The process is then followed by the mapping of data into the spatial wavenumber domain k_y using Eq. (7). Lastly, the Stolt interpolated matrix will be inverse Fourier transformed to the time domain to produce a SAR image, as shown in Fig. 7.

$$S_{mf}(k_x, k_r) = e^{jR_c\sqrt{k_r^2 - k_x^2}} \tag{6}$$

$$k_y = \sqrt{k_r^2 - k_x^2} \tag{7}$$
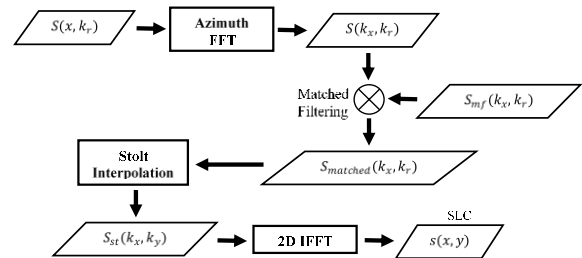
Fig. 8. Range Migration Algorithm (RMA) focusing technique.

D. InSAR Processing Tool

Interferometric SAR (InSAR) is an important technique used in GBSAR. Two SLC data sets on the same scene

measured at different observation points are required to generate a SAR interferogram. This separation in the observation points in the datasets used, known as the baseline b (as shown in Fig. 9, A_1 and A_2 being the observation points). The baseline b leads to the displacement in range Δr for each pixel between the data sets. The change in the range can be extracted from the interferogram in term of phase shift $\Delta\varphi$, as shown in Eq. (8). The phase shift $\Delta\varphi$ is useful in determining the pixel's elevation to generate the digital elevation model (DEM) of the scene. One can calculate the pixel's elevation z_p using Eq. (9). In which H is the height of the antenna, b_z and b_y being the vertical baseline in height direction and horizontal baseline in the ground range direction. For the case of a GBSAR mount at the $H = 0$ with no horizontal baseline $b_y = 0$, Eq. (9) can be rewritten into Eq. (10) as presented in [7].
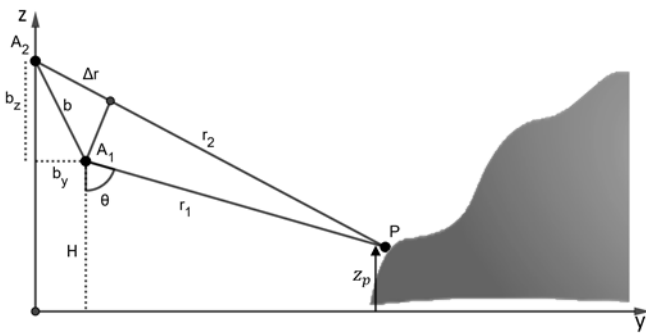
Fig. 9. InSAR geometry.

$$\Delta r = \frac{\lambda}{4\pi}\Delta\varphi \qquad (8)$$

$$h = H - \frac{r_1(\Delta r + B_h)}{B_v} \qquad (9)$$

$$z_p = \frac{r_1}{b_z}\frac{\lambda}{4\pi}\Delta\varphi \qquad (10)$$
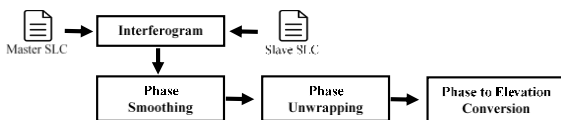
Fig. 10. Interferometric SAR (InSAR) processing.

Fig. 10 shows the flow of InSAR processing. The process started by getting the product of the Master SLC and the conjugate of the Slave SLC, where Master SLC and Slave SLC are the datasets taken from the observation points A_1 and observation points A_2 respectively. Note that there is a discontinuity in the phase value extracted from the complex interferogram. When the phase value goes beyond the extreme ends, there will be a phase jump either from $-\pi$ to $+\pi$ or from $+\pi$ to $-\pi$. This discontinuity causes the phase to be wrapped (Fig. 11a) in the between $-\pi$ and $+\pi$. Therefore, the value has to go through the phase-unwrapping process and turned into the full interferometric phase (Fig. 11b) before it can be quantified into the displacement information. Removing the

speckles in the phase image is crucial as it does affect the quality of the output phase image. Speckles can be reduced by applying the two-dimensional convolution technique before and after the phase unwrapping process. At the final stage of the InSAR process, the smoothen unwrapped interferogram will be translated into the digital elevation model (DEM), as shown in Fig 12.
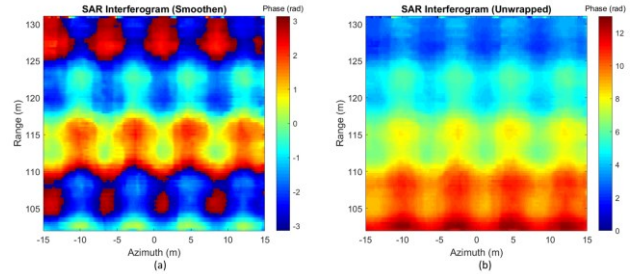
Fig. 11. SAR interferogram (wrapped and unwrapped).
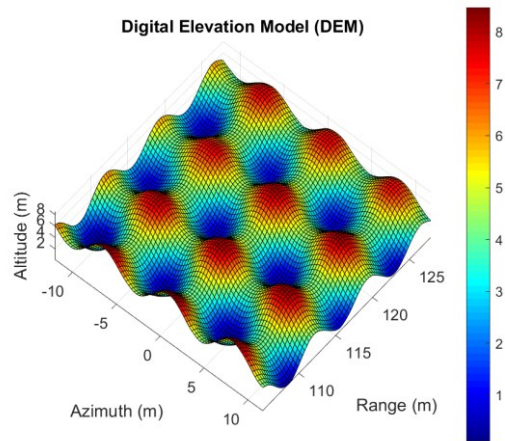
Fig. 12. Digital Elevation Model (DEM).

IV. CONCLUSION

In this paper, we have demonstrated the features of the integrated simulation and processing tool for GBSAR system (iSIM v2.0). Most of the time, point target simulation is designed solely for SAR processing algorithm test and verification purposes. GBSAR system is mainly used for deformation measurement and monitoring, which usually involves InSAR processing. The lack of the terrain's surface information in the point target signal simulation makes the data less suitable for GBSAR system test and verification. The iSIM v2.0 is explicitly developed for GBSAR. It simulates the GBSAR return signal based on both point targets and the terrain's surface information. The workflow of each of the submodules in the program, namely the virtual scene creator, SAR raw signal simulation, noise generator, SAR processing, and InSAR processing, have been presented. After some tests and verifications on each of the submodules, the preliminary result seems positive. The next stage of the project will be the validation of the program using field measurement data.

REFERENCES

[1] M. Pieraccini, M. Fratini, F. Parrini and C. Atzeni, "Dynamic Monitoring of Bridges using A High-speed Coherent Radar," *IEEE Trans. on Geoscience and Remote Sensing*, vol. 44, no. 11, pp. 3284–3288, 2006.

[2] A. Di Pasquale, G. Nico, A. Pitullo and G. Prezioso, "Monitoring Strategies of Earth Dams by Ground-based Radar Interferometry: How to Extract Useful Information for Seismic Risk Assessment," *Sensors*, vol. 18, no. 1, pp. 244, 2018.

[3] H. Liu, C. Koyama, J. Zhu, Q. Liu and M. Sato, "Post-earthquake Damage Inspection of Wood-frame Buildings by A Polarimetric GB-SAR System," *Remote Sensing*, vol. 8, no. 11, pp. 935, 2016.

[4] G. Nico, D. Leva, G. Antonello and D. Tarchi, "Ground-based SAR Interferometry for Terrain Mapping: Theory and Sensitivity Analysis," *IEEE Trans. on Geoscience and Remote Sensing*, vol. 42, no. 6, pp. 1344–1350, 2004.

[5] Z. Shao, X. Zhang and Y. Li, "Landslides Monitoring with A Squint Angle Based on GBSAR," *Progress in Electromagnetics Research*, vol. 80, pp. 13–22, 2019.

[6] G. L. Charvat, *Small and Short-range Radar Systems*. CRC Press, 2014.

[7] A. Martinez-Vazquez and J. Fortuny-Guasch, "Averaging and Formulation Impact on GB-SAR Topographic Mapping," *IEEE Geoscience and Remote Sensing Letters*, vol. 5, no. 4, pp. 635–639, 2008.